*Fibers and Polymers* 2019, Vol.20, No.2, 250-260
DOI 10.1007/s12221-019-8735-0

ISSN 1229-9197 (print version)
ISSN 1875-0052 (electronic version)

# Blood-compatible Polyaniline Coated Electrospun Polyurethane Fiber Scaffolds for Enhanced Adhesion and Proliferation of Human Umbilical Vein Endothelial Cells

**Yumei Li[1,2], Rui Zhao[3], Xiang Li[1], Chuying Wang[2]*, Huiwei Bao[2], Shudan Wang[2], Jing Fang[2], Jinqiu Huang[2], and Ce Wang[1]***

[1]*Alan G. MacDiarmid Institute, College of Chemistry, Jilin University, Changchun 130012, PR China*
[2]*Department of Clinical Pharmacy and Pharmacology of Traditional Chinese Medicine, School of Pharmaceutical Sciences, Changchun University of Chinese Medicine, Changchun 130117, PR China*
[3]*Key Laboratory of Polyoxometalate Science of the Ministry of Education, Faculty of Chemistry, Northeast Normal University, Changchun 130024, PR China*

(Received August 8, 2018; Revised November 8, 2018; Accepted November 8, 2018)

**Abstract:** The endothelialization and anti-thrombotic abilities of tissue engineered vascular scaffolds are considered to be effective properties for improving the performance small-caliber vascular scaffolds. For this purpose, we designed and developed electrically conductive fibrous scaffolds based on polyaniline coated polyurethane (PANI-PU) electrospun fibers for vascular tissue engineering applications. The porosity of PANI-PU fibers was 75.27±2.04 %. The obtained PANI-PU fibers were characterized by SEM observations, XPS analysis, water contact angle (WCA) measurement and mechanical property. The PANI functionalization aimed to improve the performance of anticoagulation and endothelialization. The WCA of PAIN-PU decreased to 35 $^{o}$ from 135 $^{o}$ of PU fibers. Blood compatibility and cytocompatibility were compared before and after PANI coating. The adhered platelet cells on PANI-PU was $6.87\times10^{5}/cm^{2}$ and plasma recalcification time was 123 s. Platelet adhesion and plasma recalcification time test showed that the PANI-PU scaffolds had a certain anticoagulant effect. The hemolysis rate of PANI-PU fibers was 0.14 %, which showed that the PANI-PU scaffolds could be used as blood contact materials. The observation of endothelial cell proliferation and morphology in human umbilical vein endothelial cells showed that PANI-PU fibers were more beneficial to cell adhesion, proliferation and extension than that of PU fibers. The results demonstrates the PANI coated electrospun PU fibers have great potential in application as small-diameter vascular grafts and this work shows new insights into conductive scaffolds for vascular tissue engineering.

**Keywords:** Electrospinning, Polyaniline, Polyurethane, Vascular scaffold

## Introduction

The emerging demand for small caliber vascular scaffolds to replace damaged vessels has attracted extensive research attention over the last few decades. Despite the significant progress in small caliber tissue engineering, inadequate endothelialization and poor hemocompatibility still limit the practical clinical applications [1,2]. Rapid *in-situ* endothelialization and good anticoagulation property of vascular grafts are considered as important factors for developing effective vascular scaffolds [3,4]. The development of a mimicking the natural extra cellular matrice (ECM) structure which is able to promote endothelialization is fundamental in the search for blood vessel substitutes in part due to their influence on cell attachment, orientation, proliferation, migration, differentiation, and final neo-tissue formation [5].

Among the many mimicking methodologies, electrospinning process is a simple, low-cost, and feasible method to fabricate one-dimensional continuous nano and micro-scale fibers, which can generate fibrous structures that imitate the microstructure of the natural ECM from diverse materials such as polymers, ceramics, and their composites [6,7]. In the electrospinning process, the precursor is fed through a spinneret. Under high voltage, precursor droplet is gradually transformed into a conical shape named a Taylor Cone; and then a charged jet is ejected from the tip of the Taylor cone and continuously stretched to form non-woven electrospun fibers on the receiver [8]. The resultant electrospun fiber mat is a good candidate for tissue engineering scaffold because of its large specific surface area, good connectivity, fiber size and similar to natural ECM [9,10]; and electrospun fibers prepared by electrospinning technology have been widely used in tissue engineering research such as skin [11], blood vessel [12], stem cells [13] and so on.

All the mentioned advantages make electrospinning an ideal method for production of vascular scaffolds. In general, vascular tissue engineering with the use of polymeric scaffolds represents a promising route in meeting the growing demand for blood vessel replacements. Various biopolymers, such as poly(ε-caprolactone) (PCL) [14], polylactic acid (PLA) [15], polyurethane (PU) [5], etc., have been electrospun into fibers to be applied in the field of biomedical materials. Among these polymers, polyurethane (PU) is broad family polymers, which has been studied

*Corresponding author: chuying820713@126.com
*Corresponding author: cwang@jlu.edu.cn

extensively in various scaffolds applications [1,16]. It is extremely interesting due to their properties such as good processability, excellent mechanical property and satisfying biocompatibility. Though some studies have used electrospun PU based fibers for vascular applications [17,18], the poor hydrophilicity of PU still presents a problem during PU's application in the manufacturing of vascular scaffolds [3,19]. Many strategies, such as blending and surface modification, have been applied to improve the hydrophilcity of PU fibers.

Surface property plays a key role in stimulating cellular interactions between cells and scaffolds as well as surface topography [20]. Recently, conductive polymers have been investigated intensively as novel functional biomaterials for improved biomedical devices due to their highly specific physicochemical and biological functions [21-23]. Moreover, conductive polymers have the function of electrical signal transfer, which can transfer external electrical stimulation to cells growing on them. Even under the conditions of no electrical stimulation, the growth and differentiation of cells are obviously improved, and the electrical activity of polymers has important influence on cell behavior. This phenomenon has caused great concern in the field of biomedicine [24,25]. Polyaniline (PANI), as one of the conductive polymers, is popular for its satisfactory performance, such as easy synthesis, environmental stability and adjustable conductivity [26]. Studies have shown that PANI has good biocompatibility in both in vitro and in vivo [27,28]. It can stimulate a variety of cellular functions, such as adhesion, proliferation, migration and differentiation [29,30]. Although several papers deal with the preparation of PANI-biopolymer electrospun composite biomaterials, only few PANI functionalized electrospun fibers are fabricated as vascular scaffolds.

Encouraged by the above description, we prepared PANI coated PU fibers via electrospinning and *in-situ* oxidative polymerization in this study. These surface functionalized fibers were evaluated by physicochemical property, blood compatibility and cytocompatibility. To our knowledge, it is the first time to systematically evaluate PANI coated electrospun PU fibers for blood vessel prosthesis. The effect of PANI on regulation of human umbilical vein endothelial cells (HUVECs) attachment and proliferation was evaluated. Moreover, in consideration of the increasing risk of thrombosis and occlusion in small-diameter vascular grafts, the hemocompatibility of the obtained fibers was also studied.

## Experimental

### Materials

Polyurethane granules (PU, Mw=8000, polyether type PU) were purchased from Sigma-aldrich. Dimethylformamide (DMF), aniline and ammonium persulfate ($(NH_4)_2S_2O_8$) were purchased from Tiantai Chemical Corp. Cell Counting Kit-8, activated partial thromboplastin time agent and prothrombin time agent were purchased from AllCells Biological Technology Co., Ltd. Phosphate buffered saline (PBS) was purchased from Beijing Dingguo Changsheng Biotechnology Co. Ltd.

### Fabrication of Electrospun PU Fibers

A PU solution (30 wt%) was obtained by dissolving PU granules in DMF. The polymer solution was loaded into a glass syringe and connected to high-voltage power supply. 18 kV potential was provided between the cathode and anode at a distance of 15 cm to prepare PU fiber film.

### Preparation of Conductive PANI Coated PU Fiber Film

To enhance the hydrophilic ability, the prepared PU electrospun fiber films were soaked in anhydrous ethanol for 1 h. During this process, the residual DMF could be also replaced by ethanol. After the treatment, the treated fiber films were used for the polymerization of PANI. The PANI functional PU fiber mat (PANI-PU) was synthesized via *in-situ* chemical oxidative polymerization technique [31]. In detail, 0.9 g $(NH_4)_2S_2O_8$ and 500 μ*l* aniline were firstly dissolved in 10 m*l* and 40 m*l* 1 M HCl respectively. Certain weight of round treated PU fibers with 18 mm in diameter were added into the aniline HCl solution, and then the $(NH_4)_2S_2O_8$ solution was added into to start the polymerization reaction, which was performed on a model BETS-M1 shaker (Kylin-Bell Lab Instruments Co., Ltd., China) with a shaking speed of 100 rpm at 20 °C for 1 h. Then, PANI-PU fiber film was washed successively with 1 M HCL, deionized water and ethanol three times, respectively. Finally, PANI-PU fiber film was dried in a vacuum oven at 40 °C for 24 h.

### Characterization of the Fibrous Scaffolds

The morphology of the fibers was characterized by a field-emission scanning electron microscopy (SEM, FEI Nova NanoSEM). The mean diameter and diameter distribution of the fibers were calculated from measuring the different parts of the fibers at 100 different fibers using the commercial software package, Image-ProPlus. The conductivity of PANI-PU fibers was measured determined by using a RTS-8 4-pointprobe resistance measurement system (Four Probe Tech., Guangzhou, China). Analysis of the X-ray photoelectron spectra (XPS) was performed on Thermo ESCALAB 250 spectrometer with a Mg-K (1253.6 eV) achromatic X-ray source. Water contact angle (WCA) test were performed at room temperature by using a contact angle analyzer (Surface Electro Optics Co., Korea) using a 4 μ*l* water droplet as the indicator. The contact angle was recorded after 5 s contact between water droplet and fibers. The mechanical properties of the fiber membranes were performed by assembling the fiber membranes (dimensions: length=40 mm, width=10-15 mm, thickness=0.15 mm) between two stainless steel clamps with a tensile speed of 20 mm·min$^{-1}$ on a mechanical strength tester (YG026H, Wuhan National Instrument Co.,

Ltd., China), according to ASTM D 882. The porosity of obtained fibers was determined by the gravimetric analysis method [32]. For this purpose, isopropyl alcohol (IPA) was used as the wetting liquid to penetrate into the pores of the membrane. Subsequently, the membrane weight was measured before and after saturated by IPA. The porosity (P) of the membrane was calculated by the following equation:

$$P(\%) = \frac{(M_I - M_d)/\rho_I}{(M_I - M_d)/\rho_I + M_d/\rho_M} \quad (1)$$

where $M_d$ is the mass of the dry membranes, $M_I$ is the mass of IPA absorbed membranes, $\rho_I$ and $\rho_M$ are the densities of isopropyl alcohol and membranes, respectively.

**Preparation of Blood Samples**

Fresh blood, obtained from a healthy wister Rat (Changchun Yis Experimental Animal Technology Co., Ltd., ethical permission letter number: 20180094), was mixed with the anticoagulant (3.8 % citrate, with a 1:9 ratio of anticoagulant to blood) to get the fresh whole anticoagulant blood. All the animal experiments were conducted in compliance with the guidelines for the care and use of laboratory animals from the National Institutes of Health, and authorize by the Ethics Committee of the Changchun University of Chinese Medicine. The whole anticoagulant blood was centrifuged at 1500 rpm for 15 min, and the resultant supernatant solution is the platelet rich plasma (PRP). Platelet-poor plasma (PPP) was obtained by centrifuging the whole anticoagulant blood at 4000 rpm for 15 min.

**Hemolysis Assay**

Fiber membrane samples (d=18 mm, weight=10 mg) were washed with 0.9 % NaCl aqueous solution and then immersed in 10 m*l* of 0.9 % NaCl aqueous solution during 30 min at 37 °C in centrifugal tube. Then 200 μ*l* of diluted fresh whole blood was added into the tubes, incubating at 37 °C for 60 min. 200 μ*l* of diluted fresh whole blood incubated with 10 m*l* of 0.9 % NaCl aqueous solution and 10 m*l* of deionized water in the absence of membrane samples were used as negative and positive controls. After centrifugation at 1500 rpm for 10 min, the absorbance of the supernatant solution at 541 nm was recorded by UV-vis spectroscopy. The hemolysis rate was calculated using the following equation (1):

$$\text{Hemolysis rate } (\%) = \frac{OD_s - OD_{nc}}{OD_{pc} - OD_{nc}} \times 100\% \quad (2)$$

in which $OD_s$, $OD_{pc}$ and $OD_{nc}$ are the absorbances of the sample, positive control, and negative control, respectively.

**Platelet Adhesion**

Blood sample preparation was illustrated in the *Supporting Information*. In brief, round membrane samples (d=18 mm) were put into 24-well plate. 200 μ*l* platelet-rich plasma (PRP) was carefully added onto each membrane and kept at 37 °C for 1 h. After washing with PBS three times, the platelet-adhered fiber membranes were fixed with 2.5 wt% glutaraldehyde solution for 2 h. Next the sample was washed with PBS and then dehydrated sequentially with 50, 70, 80, 90 and 100 % (v/v) ethanol. After drying at room temperature, the membranes were observed with SEM. The number of attached platelets on membrane surfaces was determined from the mean number of adherent platelets in ten randomly selected fields under scanning electron microscopy (SEM).

**Plasma Recalcification Time (PRT)**

The blood assays were conducted according to the previous report [33]. Round membrane samples (d=18 mm) were put into 24-well plate and platelet-poor plasma (PPP, 200 μ*l*, 37 °C) was dropped to membrane surface, and then incubated at 37 °C for 10 min. Then $CaCl_2$ aqueous solution (200 μ*l*, 0.025 M, 37 °C) was dropped to the membrane sample and the plate was gently shaken in a 37 °C water bath. Plasma recalcification time (PRT) was the time once the first fibrin strand formed. Pure PPP without samples was the control group. Each PRT value was averaged from six measurements.

**Coagulation Time Measurements**

Activated partial thromboplastin time (APTT): Round membrane samples (d=18 mm) were put into 24-well plate and then 100 μ*l* PPP was dropped to membrane surface. After incubation at 37 °C for 5 min, 100 μ*l* of APTT agent was added to the wells at 37 °C and incubated at 37 °C for another 5 min. Then, 100 μ*l* of 0.025 M $CaCl_2$ was added. Then, the coagulation time was measured as APTT value. Pure PPP without samples was the control group. All measurements were carried out six times.

Prothrombin time (PT): Round membrane samples (d= 18 mm) were put into 24-well plate and then 100 μ*l* PPP was dropped to membrane surface. After incubation at 37 °C for 3 min, 200 μ*l* of PT agent was added to the wells at 37 °C. Then, the coagulation time was measured as PT value. Pure PPP without samples was the control group. All measurements were carried out six times.

**Cell Culture**

Human umbilical vein endothelial cells (HUVECs, AllCells Biological Technology Co., Ltd. Shanghai) were cultured in complete Medium (AllCells Biological Technology Co., Ltd., hangHai). During the cell culture, the culture medium was refreshed every 2-3 days. HUVECs at passage 2-3 were used in this work. To prepare the fiber membranes for cell culture, they were put into the wells of 24-well tissue culture plate and exactly covered the well bottom. Before cell seeding, the fibrous membrane was sterilized by ultraviolet for 4 h, and then washed with PBS 3 times. Add the complete medium to soak for the night. after that remove

complete medium carefully, incubated with 0.25 % gelatin for 2 h finally. After an incubation of 2 h, the gelatin was removed carefully. HUVECs were seeded onto the fibers at a seeding density of $5\times10^4$/well. The samples were incubated at 37 °C in a humidified 5 % $CO_2$ atmosphere.

**Cellular Proliferation Assay**

$5\times10^4$/well cells were seeded onto the tissue culture polystyrene (TCP), PU fiber film and PANI-PU fiber film and allowed to incubate for 1, 3, 5 days. The viabilities of HUVECs on fibrous scaffolds were examined by CCK8 assay and fluorescence images. Before CCK8 assay, the cells were treated with the same method for parallel experiments. The CCK8 assay was performed by following these steps: at specific time intervals (1 day, 3 days, and 5 days) of cultivation, 100 μ*l* of CCK8 was added into the culture medium and the resulted solution was incubated at 37 °C for 4 h. A microplate reader was then used to measure the optical density at 450 nm. For fluorescence images, scaffolds seeded with cells for 24 h, and then incubated in 0.1 mg/m*l* Calcein AM (C3099 1 mg/m*l* solution) in PBS for 30 min at 37 °C and 5 % $CO_2$ atmosphere [34]. Tissue culture polystyrene (TCP) without any scaffolds was used as a control. The stained cells were observed using Laser scanning confocal microscopy (LSCM; FV10i, OLYMPUS, Japen).

**Cell Morphology**

To assess cell morphology as a function of nano-architectural cues, HUVECs were seeded on TCP, PU and PANI-PU scaffolds prepared under the same conditions as in the proliferation experiment. After incubation for 5 days, cells were fixed using 4 % paraformaldehyde for 10 min. Cells were permeabilized in 0.1 % Triton X-100 for 5 min. Cells were washed three times with PBS; and actin filaments stained with Rhodamine-phalloidin (Invitrogen, CA,USA) for 30 min at room temperature and dark atmosphere. After cells were washed 3 times with PBS, nuclei were stained with 4′,6-diamidino-2-phenylindole (DAPI, Sigma-aldrich) for 2-3 min. Finally, cells were washed three times with PBS and observed directly under Fluorescent Inverted microscope (FIM; iX53, OLYMPUS, Japen).

For SEM observation, the cells were incubated for 5 days, then fixed with 2.5 % gultaraldehyde, washed three times with PBS and dehydrated in a graded ethanol series (30, 50, 70, 85, 90, and 100 % respectively, each time for 20 min), and then these cells were freeze dried. Cellular morphology was visualized using scanning electron microscopy (SEM).

**Statistical Analysis**

All of the quantitative results were expressed as mean standard error of the mean. Statistical analysis was carried out by means of one-way analysis of variance (ANOVA). *p*-value less than 0.05 was considered statistically significant.

## Results and Discussion

**Morphologies**

In order to mimic the native cell ECM, PU fibers have been prepared by electrospinning technology and then polyaniline is *in-situ* oxidative polymerized on the surface of PU to provide conductivity for the regulation of HUVEC behaviors. The preparation process is shown in Figure 1. The morphologies of the PU and PANI-PU fibers are observed by SEM images (Figure 2) and the diameter distributions are also shown in Figure 2. After the electrospinning process, randomly oriented and continuous PU fibers are obtained and the surface of the fibers is smooth without the noticeable presence of beads or flat sections (Figure 2(a) and (c)). The average diameter of PU fibers is 1.45 μm (Figure 2(e)). However, PU micron fibers are hydrophobic and PANI couldn't directly deposit onto their surfaces (Figure S1). After immersion in ethanol, the hydrophilicity of PU can be improved, and then integration of PANI on the hydrophobic PU fiber surface is going on smoothly. After *in-situ* chemical oxidation polymerization of PANI, the color of the PANI-PU

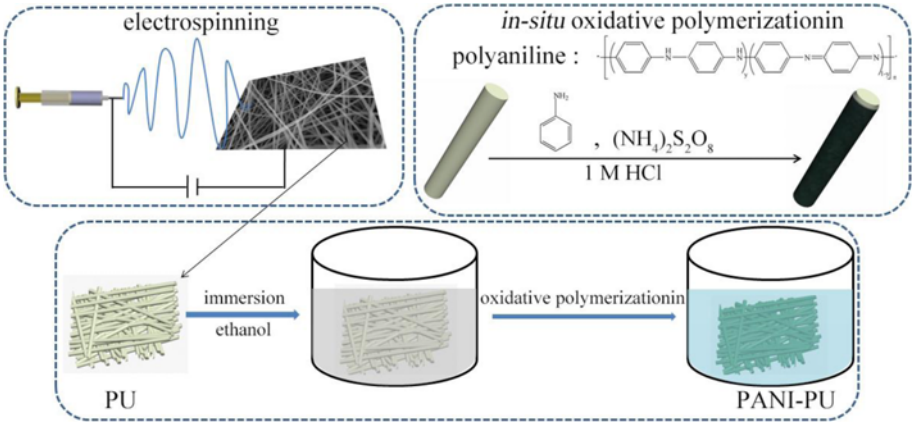


**Figure 1.** Illustration of the electrospinning process and *in-situ* oxidative polymerizationin used to fabricate PANI-PU fibers.

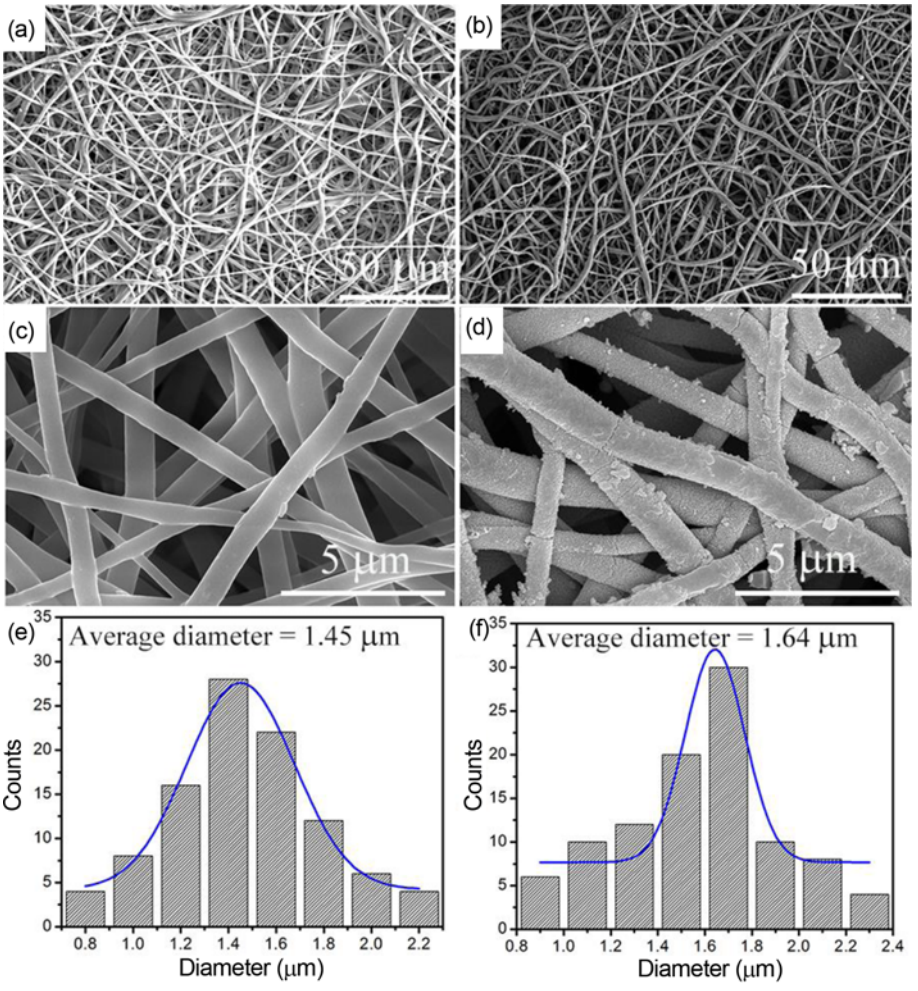


**Figure 2.** SEM images and diameter distributions of (a, c, e) PU fibers and (b, d, f) PANI-PU fibers.

fibers changes to dark green from white (Figure S2), due to the deposition of PANI. The polymerization time of PANI is determined through a preliminary study (Figure S3 and Figure S4). Many irregular particles are coated onto the surface of PU fibers leading to a much rougher surface (Figure 2(b) and (d)). The SEM observation indicates that the PANI-PU fibers are prepared successfully and PANI is coated onto the surface of PU fibers uniformly. The PANI-PU fibers still kept good fiber morphology and their fibrous structure with an average diameter of 1.64 μm (Figure 2(f)). The porosity of PU fibers is 74.18±1.68 % and the porosity of PANI-PU fibers is 75.27±2.04 %. These high porosities are beneficial to cell adhesion and proliferation. Electrical signals are essential physiological stimuli that control the adhesion and differentiation of various cell types. Thus, the electrical conductivity of a scaffold can be influence the performance and quality of a tissue engineering material. The electrical conductivity of the synthesized PANI-PU fibers is $4.66\times10^{-2}$ S/cm, which is below the reported conductivity value of pure PANI varying from approximately 1 to 100 S/cm [14]. This is because that the nonconductive component PU and the gaps between the fibers influence the conductivity. The tendency is consistent with previous reports [14,35]. This electrical activity of PANI-PU fibers would have important influence on cell behavior and could offer an excellent in-vitro platform to study effect of cell adhesion and proliferation.

**XPS Spectra**

To further examine the composition of PANI-PU fibers, XPS measurements of PU and PANI-PU fibers are used to analyze the surface composition. Both the XPS full-scan spectra of PU and PANI-PU show distinct peaks at about 285.1, 398.9 and 531.4 eV, which attribute to $C_{1s}$, $N_{1s}$ and $O_{1s}$, respectively (Figure 3(a)). The elements are consistent with the composition of PU and PANI. However, the decomposition of the $N_{1s}$ for PU and PANI-PU are different, due to the different N forms in PANI. The $N_{1s}$ spectrum of PU could be deconvoluted into only one peaks, corresponding to the -NH- (399.5 eV) of the urethane linkage (Figure 3(b))

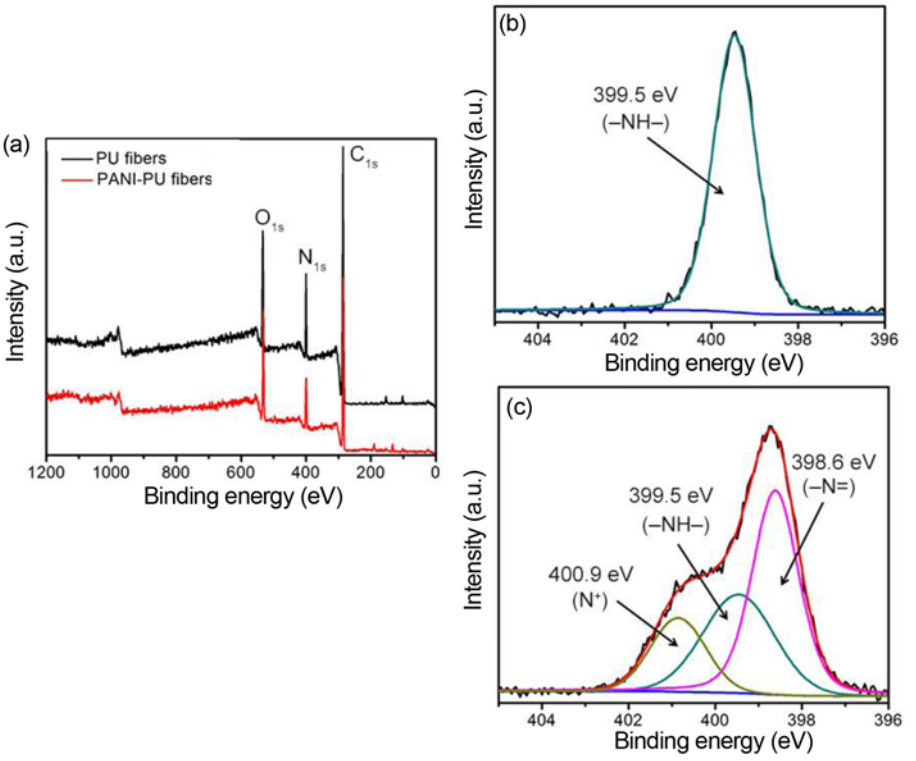


**Figure 3.** (a) XPS full-scan spectra of PU and PANI-PU fibers. High resolution peaks of $N_{1s}$ for PU fibers (b) and PANI-PU fibers (c).

[36]. After the PANI coating, the $N_{1s}$ core level signal (Figure 3(c)) in PANI-PU can be transformed into three Gaussian fitted peaks. They are centered at ~398.6 eV, ~399.5 eV and ~400.9 eV assigning to quinoid imine (-N=), benzenoid amine (-NH-) and positively charged nitrogen ($N^+$), respectively [37]. These values are in agreement with the corresponding data published for PANI. These results indicate that the PANI has been coated onto the surface of PU fibers successfully.

**Wettability and Mechanical Property**

Water contact angle measurement is used to characterize the surface relative hydrophilicity and wetting characteristics. The measured contact angle results of PU and PANI-PU fibrous mats are shown in Figure 4(a). As seen from Figure 4a, the contact angle of PU is 135.3±2.13 °, indicating its hydrophobic nature. The water droplet cannot spread well on the hydrophobic bare PU fiber scaffold surface, which is a disadvantage for cell spreading and proliferation. After the PANI coating, the contact angle significantly decreases to 35.4±3.21 °. Hydrophilicity is an important feature of tissue engineering scaffolds and surface wettability is one of the important modulators of cell shape and spreading. Good hydrophilicity provides favorable conditions for cell adhesion and spreading [38,39].

The mechanical properties of tissue engineering vascular scaffolds are quite important to evaluate whether they are

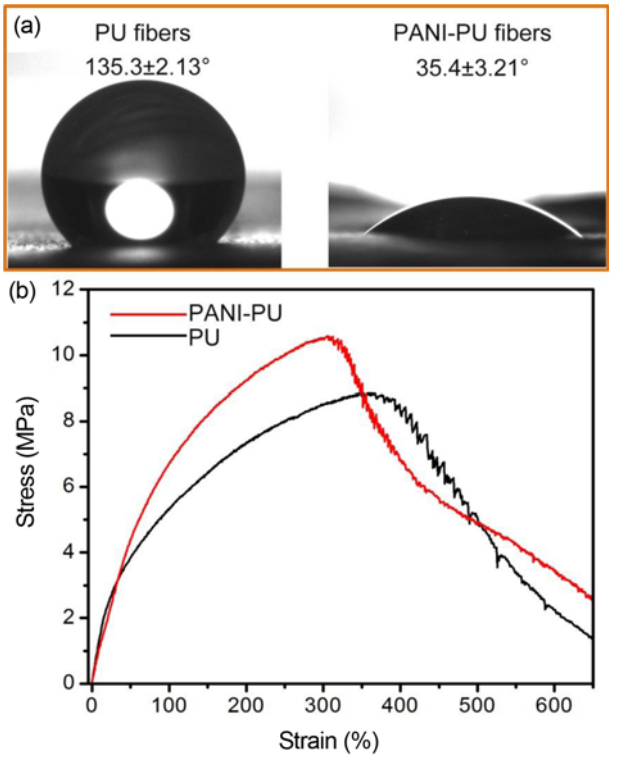


**Figure 4.** Water contact angle measurements (a) and stress-strain curves (b) of PU and PANI-PU fibers.

suitable practical application, which could tolerate bloodstream flowing force. The tensile strength of natural coronary artery is about 1.4-11.14 MPa, and elongation at break is usually above 40 % [40]. Therefore, the tensile strength and elongation at break of an artificial vascular graft should be no less than 1.4 MPa and 40 %, respectively. The mechanical properties of the PU and PANI- PU fibers are displayed in Figure 4(b). The tensile strength of pure PU fibers is 8.83± 1.02 MPa and the elongation at break is 367.16±20.56 %. After the PANI coating, the tensile strength increases to 10.56±2.12 MPa and the elongation at break has a slight decrease to 303.51±32.05 %. This is because that the loading PANI makes the fibers connect with each other more tightly, leading to an increased strength. The obtained results suggest that PANI-PU fibers could satisfy the practical requirements.

**Hemolysis Test**

It is well known that blood clotting will occur when red cells are exposed to water. Then the condition of the red cells in contact with the allogenic material will be aggravated. Hemolysis test is an important index to evaluate the blood compatibility of biomaterials [3]. Hemolysis test, as a national standard method in blood compatibility evaluation, is used to determine the degree of destruction of materials to erythrocytes. The high hemolysis rate indicates the bad blood biocompatibility. According to ISO 10993-4, materials with hemolysis values <5 % are considered as safe, which could be used as blood-contacting materials [41]. Our study finds (Figure 5(a)) that the hemolysis rate for PU fibers is 0.21 % and it is 0.14 % for PANI-PU fibers. Moreover, the hemolysis rates of polylactic acid and polycaprolactone membranes were also measured, which are 1.87 % and 2.06 %, respectively. The hemolytic ratios of PU fibers and PANI-PU fibers are both smaller than 5.0 %, which means no hemolytic activities.

**Plasma Recalcification Time (PRT) and Coagulation Time Measurements**

Plasma recalcification time (PRT) is often used to evaluate the activation of the intrinsic coagulation pathway. The principle of determination of PRT is in the absence of calcium ion plasma. The time needed for the first appearance of white filaments in plasma is measured by artificial calcium addition. It mainly reflects the inhibition effect of vascular scaffolds on coagulation system [42]. The longer the time, the lesser thrombogenic the material is. As shown in Figure 5(b), the RPT of PU and PANI-PU is respectively 110 s and 123 s. The recovery time of the latter is slightly longer than that of the former. The results indicate that the

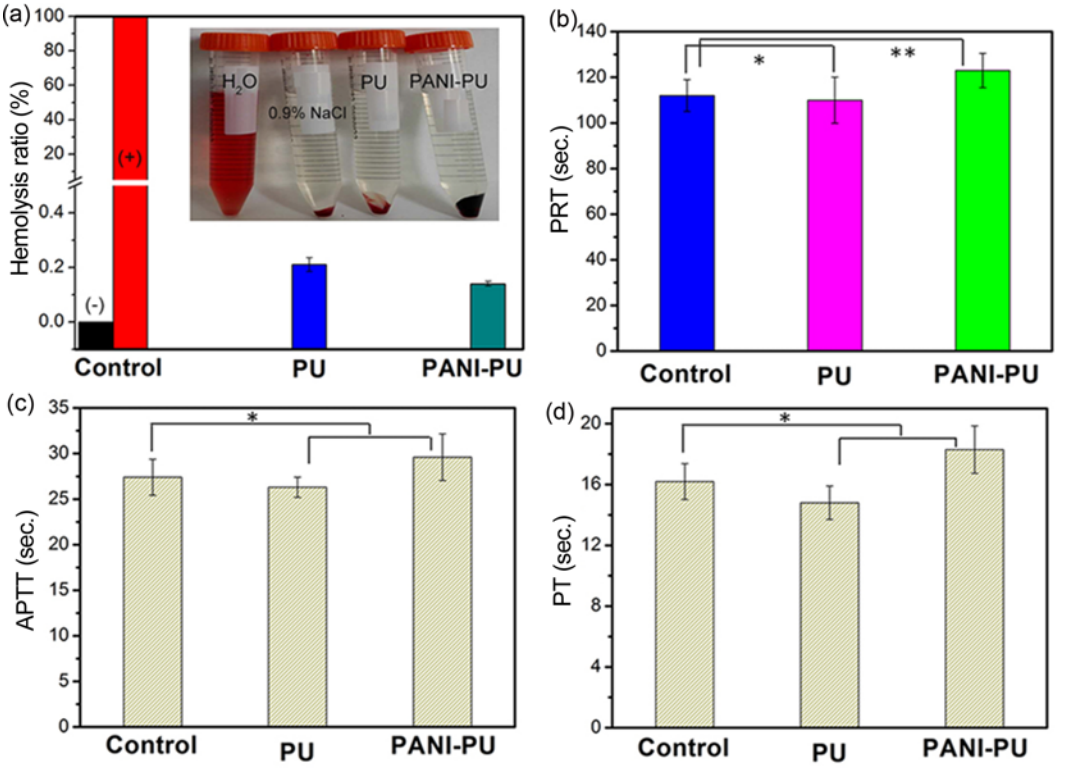


**Figure 5.** (a) Hemolysis assay for PU and PANI-PU fibers, where water and 0.9 % NaCl aqueous solution were used as positive and negative controls, respectively, (b) the plasma recalcification time (PRT) for the fibers, (c) the activated partial thromboplastin time (APTT) for the fibers, and (d) the prothrombin time (PT) for the fibers (data represent mean values±SD (n=6), *p<0.05, **p<0.01).

presence of PANI prolongs the plasma recalcification process, thus improves the anticoagulation property.

Together with plasma recalcification time (PRT), activated partial thromboplastin time (APTT) and prothrombin time (PT) were used to determine the procoagulant and anticoagulation activities of obtained fibers. The results of APTT and PT assays are shown in the following Figure 5(c) and 5(d). Compared with the control sample and PU fibers, the APTT and PT for PANI fibers were prolonged, which show a tendency similar to that of PRT. These results suggest that PANI-PU fibers possess better antithrombogenicity and blood compatibility.

**Platelet Adhesion**

It is well known that platelet adhesion and aggregation are one of the key factors to activate the coagulation pathway. The release of platelet factor from the active platelets can activate pro-thrombin to result in coagulation [43,44]. Therefore, the adhesion of platelets on the vascular scaffolds can evaluate the anticoagulant performance of the vascular scaffolds. Platelet adhesion test is also one of the indicators to evaluate the blood compatibility of biomaterials. We count the number of platelets on each fiber membrane from ten randomly selected SEM images. From the counting (Figure 6(a)) and SEM results (Figure 6(b) and 6(c)), we observe that the adhered platelet cells on PANI-PU ($6.87\times10^5/cm^2$) have an obvious reduction compared with PU ($15.63\times10^5/cm^2$). Platelets on the surface of the PANI-PU film show little aggregation, while the aggregation of platelets on PU fiber scaffolds platelets increases. These results suggest that PANI-PU fibers have good blood compatibility.

**Cellular Adhesion and Proliferation**

Materials with good biocompatibility are vital as tissue engineering materials. Biocompatibility study by considering the interactions between the obtained fibers and biological system is a crucial step to prove their practical application

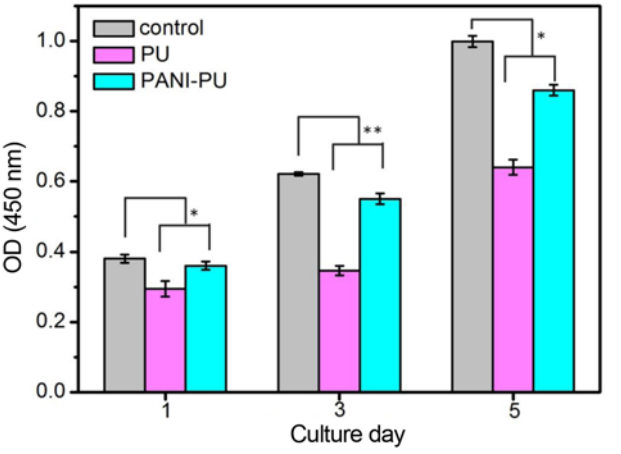


**Figure 7.** Proliferation of HUVECs on control group (TCP), PU fibers and PANI-PU fibers (data represent mean values±SD (n=8), *p<0.05, **p<0.01).

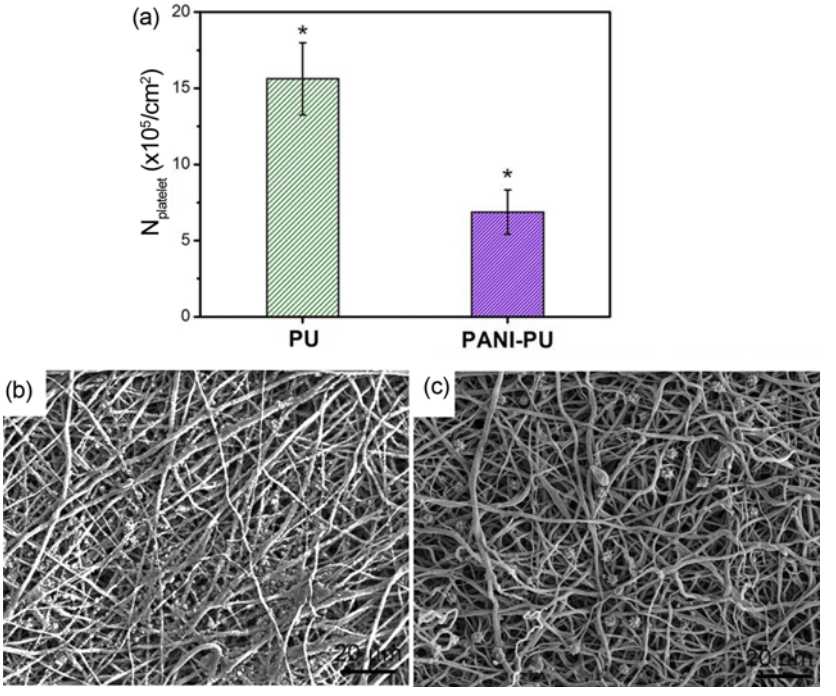


**Figure 6.** (a) The number of the adherent platelets ($N_{Platelet}$) on the fibers (data represent mean values±SD (n=6), *p<0.05). The typical SEM images of the adherent platelets on PU fibers (b) and PANI-PU fibers (c).

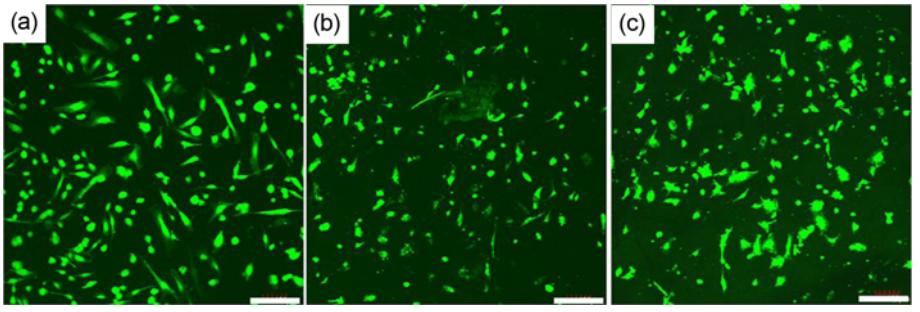


**Figure 8.** Fluorescence micrographic images of HUVECs on TCP (a), PU fibers (b) and PANI-PU fibers (c) after the incubation of 24 h (The bars are all 200 μm).

[41]. CCK8 assay was used to evaluate viability of HUVECs on PU and PANI-PU scaffolds. As shown in Figure 7, the cell viability increases as time rises. At day 1, OD values don't exhibit obvious distinctions between experimental group and control groups. While after 3 days cultivation, the proliferation of HUVECs on PANI-PU is significantly higher than that on PU. As shown in fluorescence micrographic image after 1 day (Figure 8), HUVECs successfully adhere to PANI-PU and PU fibers in comparison with control group (TCP). The better proliferation by PANI-PU in comparison with PU group was attributed to more hydrophilic and the function of PANI. Moreover, topographical features of tissue engineering constructs can also significantly influence cellular behavior. The porous structure of the electrospun fibers and the rough surface after PANI coating could provide an effective space and area for cell adhesion. PANI-coating can

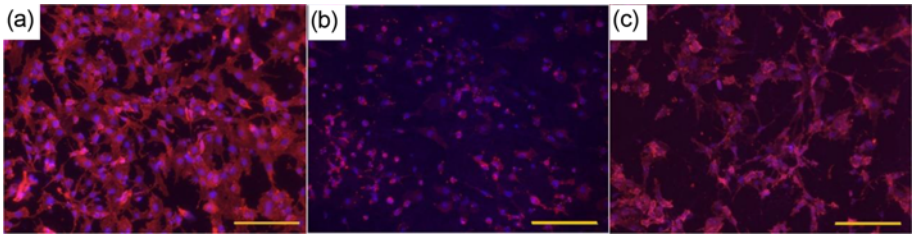


**Figure 9.** Fluorescence images of HUVECs cultured on TCP (a) PU fibers (b) and PANI-PU fibers (c) after 5 days of cell culture (the bars are all 20 μm).

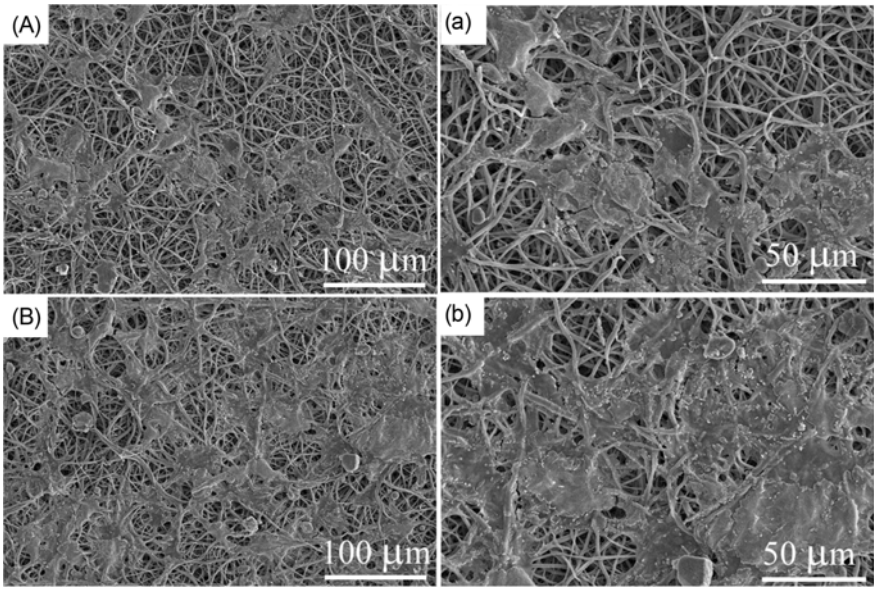


**Figure 10.** SEM micrographs of HUVECs seeded on PU fibers (A and a) and PANI-PU fibers (B and b) after 5 days of cell culture.

successfully enhance the adhesion and viability of endothelial cells on PU fibers.

**Cell Morphology**

We observed morphologies of cells grown on PANI-PU fibers and PU fibers by using cytoskeleton staining and a scanning electron microscope (Figure 9 and 10). We investigated the cytoskeleton organization of HUVECs grown on PANI-PU and PU fibers by staining the cells with rhodamine-phalloidin (Figure 9). We compared cell morphology and the organization of actin structures on different scaffold surfaces. Compared with control group (Figure 9(a)), cells grown on PU fibers display a small pherical or narrow shape and non-spreading morphology of HUVECs; and a few cells have a good extension (Figure 9(b)). Further, the cells show well-stretched actin bundles when they grow onto PANI-PU fibers (Figure 9(c)). Similar cellular morphology of HUVECs is observed via SEM images of the cells on the scaffold surfaces. The cells grown on PANI-PU fiber matrixes show flat and multipolar morphologies, but badly-stretched on PU fibers (Figure 10). These results suggest that PANI function could facilitate the cell adhesion proliferation of HUVECs on electrospun PU fibers. Therefore, it is postulated that PANI-PU fiber scaffold can be considered as a candidate of choice for small caliber vascular grafting.

## Conclusion

In this paper, we successfully prepared conductive PANI-PU scaffolds to promote endothelial cells adhesion and proliferation. PU was soaked in ethanol to improve the hydrophilicity for the polymerization of PANI. The obtained fibers were characterized by means of SEM, XPS, water contact angle measurement and mechanical property; and the coating layer of polyaniline was determined. The conductivity of PANI-PU fiber is $4.66\times10^{-2}$ S/cm. Platelet adhesion and plasma recalcification time test showed that the PANI-PU scaffolds had a certain anticoagulant effect. The hemolysis test showed that the PANI-PU scaffolds could be used as blood contact materials. The observation of endothelial cell proliferation and morphology in human umbilical vein endothelial cells showed that PANI-PU fiber was more beneficial to cell adhesion, proliferation and extension than that of PU fiber. Polyaniline coating can successfully enhance the adhesion and activity of endothelial cells onto PU fibers. The results show that the better biocompatibility and hemocompatibility make the PANI-PU fiber scaffold a more potential vascular tissue engineering material.

## Acknowledgments

This work is supported by the research grants from the National Natural Science Foundation of China (No. 51773082, 21474043 and 81173597), Jilin Provincial Industrial Innovation Program (No. 2016C024), Jilin Provincial Chinese medicine science and technology project (2017005) and Jilin provincial health and Family Planning Commission project (2016Q052).

**Electronic Supplementary Material (ESM)** The online version of this article (doi: 10.1007/s12221-019-8735-0) contains supplementary material, which is available to authorized users.

## References

1. I. Adipurnama, M. C. Yang, T. Ciach, and B. Butruk-Raszeja, *Biomater. Sci.*, **5**, 22 (2017).
2. K. Zhang, T. Liu, J. A. Li, J. Y. Chen, J. Wang, and N. Huang, *J. Biomed. Mater. Res. Part A*, **102A**, 588 (2014).
3. Z. Karahaliloğlu, *Fiber. Polym.*, **18**, 2135 (2017).
4. X. Kong, B. Han, H. Li, Y. Liang, K. Shao, and W. Liu, *J. Biomed. Mater. Res. Part A*, **100A**, 1494 (2012).
5. P. Davoudi, S. Assadpour, M. A. Derakhshan, J. Ai, A. Solouk, and H. Ghanbari, *Mat. Sci. Eng. C*, **80**, 213 (2017).
6. B. K. Shrestha, S. Shrestha, A. P. Tiwari, J. I. Kim, S. W. Ko, H. J. Kim, C. H. Park, and C. S. Kim, *Mater. Des.*, **133**, 69 (2017).
7. C. J. Mortimer and C. J. Wright, *Biotechnol. J.*, **12**, 600693 (2017).
8. K. Kim, M. Kang, I. J. Chin, and H. J. Jin, *Macromol. Res.*, **13**, 533 (2005).
9. Z. Cai, C. Zhu, J. Guo, Q. Zhang, and K. Zhao, *Mat. Sci. Eng. C*, **82**, 29 (2018).
10. M. Salehi, A. Vaez, M. Naseri-Nosar, S. Farzamfar, A. Ai, J. Ai, S. Tavakol, M, Khakbiz, and S. Ebrahimi-Barough, *Fiber. Polym.*, **19**, 125 (2018).
11. A. R. Sadeghi-avalshahr, M. Khorsand-Ghayeni, S. Nokhasteh, A. M. Molavi, and H. Naderi-Meshkin, *J. Mater Sci: Mater. Med.*, **28**, 14 (2017).
12. H. Wang, Y. Feng, H. Zhao, R. Xiao, J. Lu, L. Zhang, and J. Guo, *Macromol. Res.*, **20**, 347 (2012).
13. S. M. Damaraju, Y. Shen, E. Elele, B. Khusid, A. Eshghinejad, J. Li, M. Jaffe, and T. L. Arinzeh, *Biomaterials*, **149**, 51 (2017).
14. Y. Li, X. Li, R. Zhao, C. Wang, F. Qiu, B. Sun, H. Ji, J. Qiu, and C. Wang, *Mat. Sci. Eng. C*, **72**, 106 (2017).
15. J. H. Kim, T. H. Kim, G. Z. Jin, J. H. Park, Y. R. Yun, J. H. Jang, and H. W. Kim, *J. Biomed. Mater. Res. Part A*, **101A**, 1447 (2013).
16. A. Burke and N. Hasirci, *Adv. Exp. Med. Biol.*, **553**, 83 (2004).
17. A. Abdalhay, M. Bartnikowski, S. Hamlet, and S. Ivanovski, *Mat. Sci. Eng. C*, **82**, 10 (2018).
18. Z. Zaredar, F. Askari, and P. Shokrolahi, *Prog. Biomater*. https://doi.org/10.1007/s40204-018-0101-6 (2018).

19. R. Subramaniam, M. P. Mani, and S. K. Jaganathan, *Cardiovasc. Eng. Techn*., **9**, 503 (2018).
20. P. Ferreira, P. Alves, P. Coimbra, and M. H. Gil, *J. Coat. Technol. Res.*, **12**, 463 (2015).
21. H. Shokry, U. Vanamo, O. Wiltschka, J. Niinimäki, M. Lerche, K. Levon, M. Lindend, and C. Sahlgren, *Nanoscale*, **7**, 14434 (2015).
22. J. Tan, Z. Xie, Z. Zhang, Y. Sun, W. Shi, and D. Ge, *J. Mater. Sci.*, **53**, 447 (2018).
23. S. Hosseinzadeh, S. M. Rezayat, E. Vashegani-Farahani, M. Mahmoudifard, S. Zamanlui, and M. Soleimani, *Polymer*, **97**, 205 (2016).
24. S. Hosseinzadeh, M. Mahmoudifard, F. Mohamadyar-Toupkanlou, M. Dodel, A. Hajarizadeh, M. Adabi, and M. Soleimani, *Bioprocess Biosyst. Eng.*, **39**, 1163 (2016).
25. Y. Zou, J. Qin, Z. Huang, G. Yin, X. Pu, and D. He, *ACS Appl. Mater. Interfaces*, **8**, 12576 (2016).
26. T. H. Qazi, R. Rai, and A. R. Boccaccini, *Biomaterials*, **35**, 9068 (2014).
27. P. R. Bidez, S. Li, A. G. Macdiarmid, E. C. Venancio, Y. Wei, and P. I. Lelkes, *J. Biomat. Sci. Polym. E*., **17**, 199 (2006).
28. S. Liu, J. Wang, D. Zhang, P. Zhang, J. Ou, B. Liu, and S. Yang, *Appl. Surf. Sci.*, **256**, 3427 (2010).
29. G. Thrivikraman, G. Madras, and B. Basu, *Biomaterials*, **35**, 6219 (2014).
30. M. Y. Li, P. Bidez, E. Guterman-Tretter, Y. Guo, A. G. MacDiarmid, P. I. Lelkes, and C. X. Song, *Chinese J. Polym. Sci.*, **25**, 331 (2007).
31. J. Wang, K. Pan, E. P. Giannelis, and B. Cao, *RSC Adv.*, **3**, 8978 (2013).
32. R. Zhao, X. Li, B. Sun, Y. Li, Y. Li, R. Yang, and C. Wang, *J. Mater. Chem. A*, **5**, 1133 (2017).
33. J. Zhang, C. Liu, F. Feng, D. Wang, S. Lu, G. Wei, H. Mo, and T. Qiao, *Colloid. Surface B*, **160**, 192 (2017).
34. R. B. Montero, X. Vial, D. T. Nguyen, S. Farhand, M. Reardon, S. M. Pham, and F. M. Andreopoulos, *Acta Biomater.*, **8**, 1778 (2012).
35. C. Basavaraja, D. G. Kim, and W. J. Kim, *Bull. Korean Chem. Soc*., **32**, 927 (2011).
36. P. C. Rodrigues, P. N. Lisboa-Filho, A. S. Mangrich, and L. Akcelrud, *Polymer*, **46**, 2285 (2005).
37. S. Bai, Y. Zhao, J. Sun, Z. Tong, R. Luo, D. Li, and A. Chen, *Sens. Actuators. B*, **239**, 131 (2017).
38. B. D. Bovan, T. W. Hummert, D. D. Dean, and Z. Schwartz, *Biomaterials*, **17**, 137 (1996).
39. C. J. Pan, Y. Hou, Y. N. Wang, F. Gao, T. Liu, Y. H. Hou, Y. F. Zhu, W. Ye, and L. R. Wang, *Mat. Sci. Eng. C*, **67**, 132 (2016).
40. L. Yu, Y. Feng, Q. Li, X. Hao, W. Liu, W. Zhou, and W. Zhang, *React. Funct. Polym.*, **91**, 19 (2015).
41. Z. Peng, Y. Yang, J. Luo, C. Nie, L. Ma, C. Cheng, and C. Zhao, *Biomater. Sci.*, **4**, 1392 (2016).
42. D. Motlagh, J. Yang, K. Y. Lui, A. R. Webb, and G. A. Ameer, *Biomaterials*, **27**, 4135 (2006).
43. M. C. Serrano, R. Pagani, J. Peña, M. Vallet-Regí, J. V. Comas, and M. T. Portolés, *J. Tissue Eng. Regen. Med.*, **5**. 238 (2011).
44. P. Davoudi, S. Assadpour, M. A. Derakhshan, J. Ai, A. Solouk, and H. Ghanbari, *Mat. Sci. Eng. C*, **80**, 213 (2017).